THE JOURNAL OF BIOLOGICAL CHEMISTRY VOL. 288, NO. 25, pp. 18093–18103, June 21, 2013
Published in the U.S.A.

Characterization and Favorable *in Vivo* Properties of Heterodimeric Soluble IL-15·IL-15Rα Cytokine Compared to IL-15 Monomer*[S]

Received for publication, February 20, 2013, and in revised form, May 2, 2013 Published, JBC Papers in Press, May 6, 2013, DOI 10.1074/jbc.M113.461756

Elena Chertova[‡1], Cristina Bergamaschi[§1], Oleg Chertov[¶], Raymond Sowder[‡], Jenifer Bear[‖], James D. Roser[‡], Rachel K. Beach[§‖], Jeffrey D. Lifson[‡], Barbara K. Felber[‖], and George N. Pavlakis[§2]

From the [‡]AIDS and Cancer Virus Program and the [¶]Protein Chemistry Laboratory, Advanced Technology Program, SAIC-Frederick Inc., Frederick National Laboratory, Frederick, Maryland 21702 and the [§]Human Retrovirus Section, Vaccine Branch, Center for Cancer Research, and the [‖]Human Retrovirus Pathogenesis Section, Vaccine Branch, Center for Cancer Research, National Cancer Institute, Frederick, Maryland 21702

Background: IL-15 acts *in vivo* in association with IL-15Rα, as a heterodimeric cytokine.
Results: Authentically processed and glycosylated IL-15·sIL-15Rα heterodimer was purified from human cells and characterized by sequencing and functional studies.
Conclusion: IL-15 heterodimer shows favorable *in vivo* properties compared with monomeric IL-15.
Significance: Characterization and availability of the IL-15 heterodimer is important for functional studies and clinical applications.

Interleukin-15 (IL-15), a 114-amino acid cytokine related to IL-2, regulates immune homeostasis and the fate of many lymphocyte subsets. We reported that, in the blood of mice and humans, IL-15 is present as a heterodimer associated with soluble IL-15 receptor α (sIL-15Rα). Here, we show efficient production of this noncovalently linked but stable heterodimer in clonal human HEK293 cells and release of the processed IL-15·sIL-15Rα heterodimer in the medium. Purification of the IL-15 and sIL-15Rα polypeptides allowed identification of the proteolytic cleavage site of IL-15Rα and characterization of multiple glycosylation sites. Administration of the IL-15·sIL-15Rα heterodimer reconstituted from purified subunits resulted in sustained plasma IL-15 levels and in robust expansion of NK and T cells in mice, demonstrating pharmacokinetics and *in vivo* bioactivity superior to single chain IL-15. These identified properties of heterodimeric IL-15 provide a strong rationale for the evaluation of this molecule for clinical applications.

IL-15 is a common γ chain cytokine highly related to IL-2 with a nonredundant role in the development, survival, proliferation, and activation of lymphocytes, including NK cells, $CD8^+$ T-cells, and intestinal intraepithelial lymphocytes (1–5). Due to these properties, and the beneficial effects of its administration in several preclinical cancer models (6–12), IL-15 has been proposed for use in cancer immunotherapy (13–15).

IL-15 acts on the surface of the cell in complex with membrane-embedded IL-15Rα to engage the IL-2·IL-15 receptor β/γ complex on nearby cells, a process termed trans-presentation (16). Genetic and cell transfer experiments suggested that the simultaneous expression of IL-15Rα in the same cell is necessary for the production and secretion of IL-15 under physiological conditions (17–20). We demonstrated that co-expression of the two molecules in the same mammalian cell leads to rapid intracellular association of IL-15 and IL-15Rα in the endoplasmic reticulum, stabilization of both molecules, and efficient transport of the heterodimeric complex to the cell surface, where it is bioactive (21, 22). In addition, the surface heterodimer is rapidly cleaved and released in the plasma as bioactive IL-15·sIL-15Rα cytokine (22). These results demonstrated that IL-15 and IL-15Rα are coproduced and form heterodimers, and that the active form of IL-15 found in the body is the heterodimer in two distinct forms, either cell associated or soluble. Recently, we demonstrated that the circulating form of IL-15 in biological fluids is indeed in complex with soluble IL-15Rα (sIL-15Rα)[3] in both mouse and human (23). These findings provide additional support to previous works reporting the ability of recombinant sIL-15Rα to act as potent agonist of IL-15 function *in vivo* (6, 10, 22, 24, 25), and suggest that the IL-15·IL-15Rα heterodimeric form is responsible for IL-15 bioactivity. The molecular mechanism of expression and function of IL-15·IL-15Rα and its *in vivo* persistence appear unique among the γ chain family of cytokines and suggest that IL-15·sIL-15Rα may provide important advantages over monomeric IL-15 for clinical use.

The mechanism responsible for shedding of the heterodimer from the cell surface is poorly understood and the C terminus sequence of naturally cleaved sIL-15Rα is unknown. For these

* This work was supported by the Intramural Research Program, National Cancer Institute, National Institutes of Health (NCI/National Institutes of Health) and federal funds from the National Cancer Institute, National Institutes of Health, under contract number HHSN261200800001E.
[S] This article contains supplemental Figs. S1–S6 and Tables S1 and S2.
[1] Both authors contributed equally to this work.
[2] To whom correspondence should be addressed: Human Retrovirus Section, Vaccine Branch, Center for Cancer Research, National Cancer Institute, Frederick, MD. E-mail: pavlakig@mail.nih.gov.

[3] The abbreviations used are: IL-15·sIL-15Rα, soluble heterodimer of IL-15 and extracellular fragment of IL-15 receptor α; Fx, fraction; HexNAc, *N*-acetylhexosamine; CFSE, carboxyfluorescein succinimidyl ester.

reasons, the molecular characterization of the bioactive heterodimeric cytokine is important. Isolation of the heterodimer from human tissues is difficult, because of the small quantities of circulating cytokine (26). We therefore developed methods for production and purification of IL-15·IL-15Rα heterodimers synthesized, processed, and secreted by human cells after gene transfer. We developed stable, clonal HEK293-derived human cell lines overproducing naturally processed IL-15·sIL-15Rα heterodimers and an efficient purification procedure to yield biologically active heterodimeric IL-15·sIL-15Rα cytokine. This also allowed the characterization of the IL-15·sIL-15Rα complexes, determination of the amino acid sequence, and the proteolytic cleavage site of the sIL-15Rα, analysis of the glycosylation, and evaluation of pharmacokinetics and *in vivo* bioactivity.

EXPERIMENTAL PROCEDURES

Generation of Mammalian Cell Lines Overproducing Heterodimeric IL-15·IL-15Rα—DNA vectors optimized for the efficient expression of human IL-15 and full-length IL-15Rα (22, 27) were used for the generation of stable clonal cell lines. Highly purified, endotoxin-free DNA plasmid (Qiagen EndoFree Giga kit, Hilden, Germany) was linearized by restriction enzyme digestion and purified using the Nucleotide Removal Kit (Qiagen) and ethanol precipitated under sterile conditions. HEK293 cells (Invitrogen, number 11631017) were stably transfected by the calcium phosphate coprecipitation technique using optimized plasmids. Clones 19.7 and 1.5 were among the highest producers of IL-15·sIL-15Rα. Another HEK293-derived human cell line (clone 2.66) producing IL-15·sIL-15Rα heterodimers was generated using DNA vectors expressing IL-15 and the extracellular region of IL-15Rα (truncated sIL-15Rα, aa 1–175 (22, 28) of the mature molecule). The cells were expanded and seeded in serum-free media in a hollow fiber system (FiberCell Systems Inc). Glucose consumption was measured daily and serum-free media was replaced when the glucose concentration dropped below 100 mg/dl. Cell supernatants (20 ml) were harvested daily for up to 5 months and assayed for IL-15 levels by ELISA (R&D Systems).

Reverse Phase-High Performance Liquid Chromatography (RP-HPLC) Separation and Analysis of IL-15 Heterodimers—For analytical RP-HPLC, samples were centrifuged to pellet cellular debris and 100 μl of media containing IL-15·sIL-15Rα complexes were separated by RP-HPLC under nonreducing conditions at a flow rate of 0.3 ml/min on 2.1 × 100-mm Poros® R2/10 column (ABI, USA), using aqueous acetonitrile/trifluoroacetic acid solvents and a Shimadzu HPLC system equipped with LC-10AD pumps, an SCL-10A system controller, a CTO-10AC oven, an FRC-10A fraction collector, and an SPD-M10AV diode array detector at 55 °C. Buffer A was 0.1% trifluoroacetic acid (TFA) in water. The column was equilibrated with 10% buffer B (0.1% TFA in acetonitrile). The gradient of buffer B was: 10–43%, 9 min; 43–44%, 12 min; 44–85%, 4 min; 85%, 5 min. Peaks were detected by UV absorption at 206 and 280 nm. Quantitation of purified proteins was performed by amino acid analysis using a Hitachi L-8800 Amino Acid Analyzer. Purified IL-15 and sIL-15Rα subunits were mixed at a 1:1 molar ratio to allow re-association of complexes. Analysis of reconstituted IL-15·sIL-15Rα complexes was performed in both denaturing and nondenaturing conditions on polyacrylamide gels (12 and 4–20% gradient, respectively), and visualized by Coomassie Blue staining. Formation of the complexes was confirmed by Western immunoblot analysis, using anti-human IL-15 or anti-human IL-15Rα antibodies (AF315 and AF247, respectively, R&D Systems).

Preparative RP-HPLC was performed using a Dionex HPLC system equipped with Ultimate 3000 Binary pumps model number HPG-3400A, Ultimate 3000 Photodiode Array Detector model number PDA-3000, Ultimate 3000 Column Compartment model number TCC-3000, Ultimate 3000 Solvent Rack and Degasser model number SRD-3400, Isco Fraction Collector, model number Foxy 200. Typically, 20 ml/run were loaded directly on the column after centrifugation to remove cell debris.

Initial purification was performed on Waters RCM 25 × 100-mm uBondapak-C18 column at a flow rate of 5 ml/min at room temperature. Buffer A was 0.1% TFA in water. The gradient of buffer B was: 20–32%, 60 min; 32–47%, 40 min; 47–55%, 1 h 20 min; 55–65%, 20 min; 65–90%, 20 min; and 90%, 10 min. The fractions corresponding to sIL-15Rα and IL-15 were pooled separately and further purified by RP-HPLC under nonreducing conditions. Further purification of sIL-15Ra was done on 16 × 100-mm POROS R2/10 column at 26.0 °C and flow rate 5 ml/min. The gradient of buffer B was: 5–15%, 10min; 15–32%, 120 min; 32–100%, 20 min; 100%, 10 min.

For further purification of IL-15, fractions corresponding to IL-15 were pooled and re-purified first on 16 × 100-mm POROS R2/10 at 26 °C at flow rate 5 ml/min. The gradient of buffer B was: 20–36%, 30 min; 36–50%, 150 min; 50–90%, 20 min; 90%, 10 min. Peaks were detected at 206 and 280 nm and analyzed by sequencing using an automated Applied Biosystems Inc. 477 Protein Sequencer, by SDS-polyacrylamide gel electrophoresis (PAGE), and by immunoblot analysis using an Enhanced Chemiluminescence (ECL) procedure (Amersham Biosciences Life Science). Quantitation of total protein in mixtures or purified subunits was done by amino acid analysis using a Hitachi L-8800 Amino Acid Analyzer. The sIL-15Rα and IL-15 pools were mixed in equimolar quantities and lyophilized.

Proteolytic Digestion to Identify C Terminus of sIL-15Rα—60 μg of naturally cleaved sIL-15Rα were dissolved in 0.02 M Tris-HCl, pH 8.5, and Lys-C endoproteinase (Roche Applied Science Gmbh, Mannheim, Germany) (20:1 (w/w) protein-protease) was added and incubated for 22 h at 37 °C. After digestion, reverse-phase HPLC separation of Lys-C fragments were performed under nonreducing conditions on a 2.1 × 100-mm Vydac C18 column at 0.3 ml/min, using a Shimadzu HPLC system. The gradient of buffer B was: 7–30%, 25 min; 30–70%, 5min; 70%, 5 min at 55 °C. Peaks were detected at 206 and 280 nm and analyzed by sequencing using an automated Applied Biosystems Inc. 477 A protein sequencer.

MALDI-TOF MS—Aliquots of HPLC fractions were mixed with equal volume of matrix solution (α-cyano-4-hydroxycinnamic acid), and 1.5 μl of mixture was spotted on a target plate and analyzed by MALDI-TOF MS (matrix-assisted laser desorption ionization time-of-flight mass spectrometry) on Ultra-

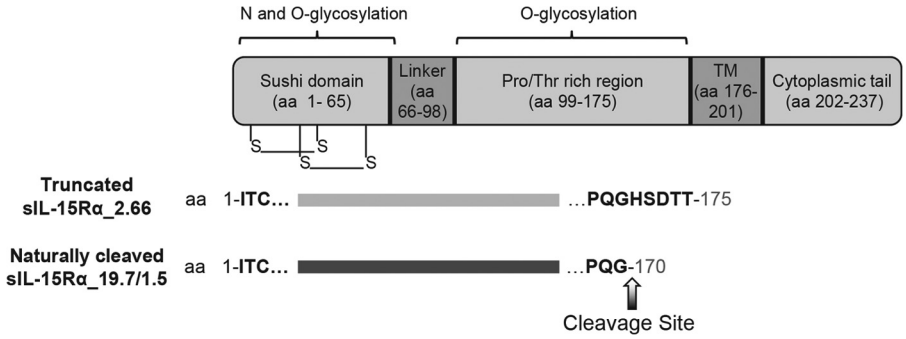

FIGURE 1. **Schematic representation of mature IL-15Rα.** The different domains of mature IL-15Rα are shown (the 30-amino acid long signal peptide is not included). The sushi domain forms 2 disulfide bonds and is characterized by several *N*- and *O*-glycosylation sites (HexNAc on Ser-8, -18, -20, -23, and -31 as reported in supplemental Fig. S5 and S6). The Pro/Thr-rich domain contains *O*-glycosylation at Thr-156 or Ser-158 (as reported in supplemental Fig. S4). Truncated sIL-15Rα_2.66 comprises 175 amino acids. Naturally cleaved sIL-15Rα from both clones 19.7 and 1.5 comprise 170 amino acids; the *arrow* indicates the cleavage site upon expression of IL-15Rα on the cell membrane.

flex III TOF/TOF (Bruker Daltonics, Billerica, MA). Spectra were externally calibrated in reflector mode using Bruker Peptide Calibration Standard II. Monoisotopic masses were determined using FlexAnalysis 3.3 (Bruker Daltonics) with the SNAP peak picking algorithm. The spectra were analyzed using BioTools 3.2 software (Bruker Daltonics). Mass spectrometric sequencing of particular peptides was performed by MALDI-TOF MS/MS analysis in the "LIFT" mode with manual selection of precursor ions. Fragment ion spectra were used for SwissProt protein database search by the Mascot MS/MS ion search program on the NIH Mascot server. The obtained identifications were confirmed by comparing the BioTools generated fragment ions series with experimental MS/MS data. Confidence in the identification was assessed based on the Mascot Protein or Ion score, which is $-10 \times \log(P)$, where P is the probability that the observed match is a random event. In-Source Decay MALDI-TOF analysis of intact HPLC-purified sIL-15Ra was done using 1,5-diaminonaphthalene as matrix as suggested by in Bruker's technical note number TN-36 (automated acquisition of in-source decay MALDI spectra for the N- and C-terminal sequence determination of intact proteins). MS/MS tolerance in analysis of In-Source Decay spectrum using BioTools was 1.5 Da. Mass spectrometry of the sIL-15Rα preparation was performed on an Applied Biosystems Voyager-DE Pro time-of-flight mass spectrometer operated in linear mode under positive ion conditions. Typical voltages were 25 kV accelerating, guide wire 0.15%, and grid voltage 91.5%. A nitrogen laser was used at 337 nm with 250 laser shots averaged per spectrum. A CovalX HM-1 high mass detector was used with HV-1 set to 2.5 kV and HV-2 at 20 kV. Bovine serum albumin and apo-myoglobin were used as standards for external calibration. Sinapic acid was used as matrix. Data analysis was carried out using "Data Explorer" software resident on the Voyager mass spectrometer.

IL-15 Treatment in Mice—Six-week-old female C57BL/6 mice were obtained from Charles River Laboratories, Inc. (Frederick, MD). *Escherichia coli*-derived monomeric IL-15 (29) and purified IL-15 heterodimers were injected at a dose of 3 μg of IL-15 eq/mouse intraperitoneally. Mice were bled at different time points after protein injection, and the serum IL-15 levels were measured using human IL-15 chemiluminescent immunoassay (Quanti-Glo, R & D Systems).

CFSE Labeling of Cells and Cell Adoptive Transfer in Mice—To make single cell suspensions, spleens from 6-week-old female C57BL/6 mice were gently squeezed through a 100-μm Cell Strainer (Thomas) and washed in RPMI 1640 medium (Invitrogen) to remove any remaining organ stroma. Cells were incubated for 10 min at 37 °C with CFSE (2 μM; Molecular Probes) and washed twice. CFSE-labeled cells (20×10^6) were resuspended in PBS and injected intravenously into congenic mice. IL-15 treatment was performed the day after cell injection. At day 4, mice were sacrificed and splenocytes were analyzed by multiparameter flow cytometry to evaluate the bioactivity of IL-15. Briefly, the cells were washed in FACS buffer containing 0.2% fetal calf serum and stained with the following panel of conjugated rat anti-mouse antibodies: CD3-APCCy7, CD4-PerCP, CD8-Pacific Blue, and NK1.1-PeCy7 or -APC (BD Biosciences). The percentage of cells of the original population that had divided in response to IL-15 treatment was calculated based on CFSE intensity. Samples were acquired using a LSRII flow cytometer (BD Biosciences), and the data were analyzed by FlowJo software (Tree Star, San Carlos, CA). In some experiments, surface staining of cells was followed by intracellular staining with Ki-67 antibody (BD Biosciences) for the detection of proliferating cells.

RESULTS

Generation of Human Cell Lines Producing High Levels of IL-15·sIL-15Rα—We previously reported the generation of optimized combination vectors for the coordinate expression of the two chains of the human heterodimeric cytokine IL-15·IL-15Rα (21, 22). Yields of secreted bioactive IL-15 achieved by these plasmids were >1,000-fold higher compared with wt IL-15 cDNAs (22, 27). These plasmids were used to develop stable clonal IL-15·sIL-15Rα-producing human HEK293 cell lines. We used intact genes of IL-15 and IL-15Rα for the generation of these cell lines. Membrane-bound IL-15Rα is composed of 5 domains, the sushi domain responsible for the binding to IL-15, a linker region, the Pro/Thr-rich domain, the transmembrane domain and cytoplasmic tail (30, 31) (Fig. 1). Upon stable introduction of the genes into HEK293 cell lines, the heterodimer was obtained in the culture supernatant in a soluble form, after transport of the IL-15·IL-15Rα to the plasma membrane and proteolytic cleavage of the extracel-

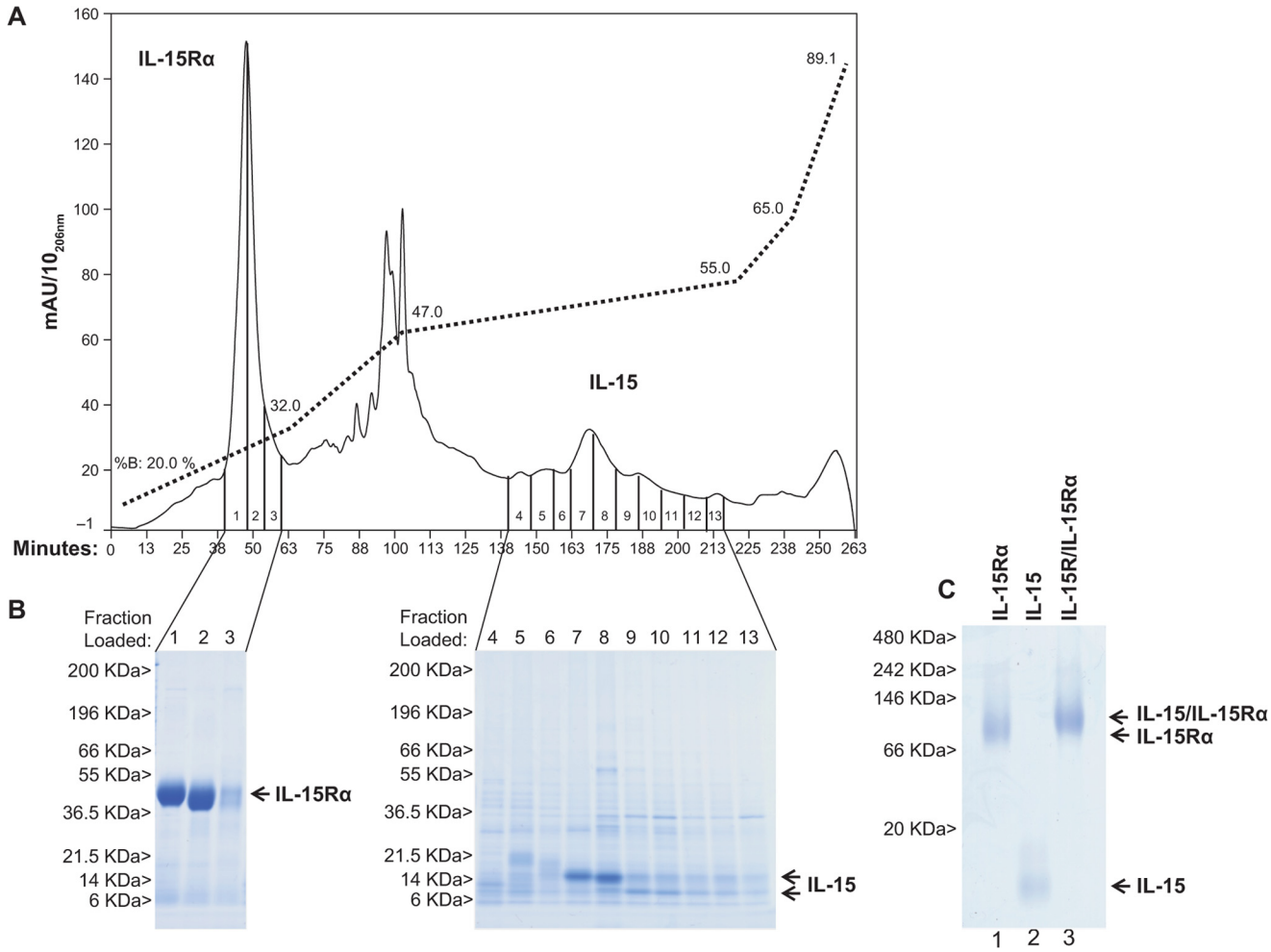

FIGURE 2. **Production and purification of human IL-15·sIL-15Ra.** *A,* HPLC purification of IL-15·sIL-15Rα heterodimers from HEK293-derived human cell line 19.7. *B,* proteins were eluted from the column and analyzed by SDS-PAGE. *C,* After final purification (see supplemental Fig. S2, *A–D*) IL-15, sIL-15Rα, and the re-constituted IL-15·sIL-15Rα heterodimer (at a 1:1 molar ratio) were visualized on native PAGE.

lular part of IL-15Rα by cellular enzymes. The mature secreted IL-15Rα molecule is depicted in Fig. 1. Clones 19.7 and 1.5 were selected as the highest producers of IL-15·sIL-15Rα heterodimers. Both stable clones were grown in continuous culture in serum-free medium, using a hollow fiber culture system, and the supernatants were harvested daily. Clone 19.7 produced 70 mg of IL-15/liter (calculated as monomer IL-15 by ELISA) for up to 5 months (supplemental Fig. S1*A*). HPLC analysis under nonreducing conditions of weekly samples of supernatants produced by clone 19.7 collected from day 29 through day 137 in the bioreactor demonstrated stable production of IL-15·sIL-15Rα heterodimer over this interval (supplemental Fig. S1*B*). Similar results were obtained for clone 1.5. These results demonstrated that high levels of IL-15·sIL-15Rα heterodimeric cytokine production were achieved in stable human HEK293-derived cell lines. We have previously reported the generation of a DNA vector encoding the extracellular portion of IL-15Rα (22) (truncated sIL-15Rα, encoding the signal peptide and 175 amino acids of the mature IL-15Rα, Fig. 1). We established an additional cell line (clone 2.66) producing the engineered IL-15·sIL-15Rα complexes after transfer of genes encoding IL-15 and the truncated sIL-15Rα form. The known C terminus sequence of truncated sIL-15Rα generated from clone 2.66 (Fig. 1) was used as control for the identification of the natural cleavage site on IL-15Rα after expression of the full-length molecule on the cell membrane (see below).

Purification IL-15·sIL-15Rα by HPLC Under Nonreducing Conditions—We employed a purification strategy using reverse-phase HPLC (RP-HPLC) under nonreducing conditions, which keeps intact the disulfide bonds of the noncovalently associated IL-15 and sIL-15Rα subunits but dissociates the subunits from each other. The chains were purified and characterized separately, and they were subsequently re-associated *in vitro* at a 1:1 molar ratio to regenerate the intact heterodimeric cytokine. The first purification step was performed using Waters RCM 25 × 100-mm μBondapak C18 column, with the IL-15 and sIL-15Rα subunits dissociating in the acetonitrile containing buffer used for separation. Fig. 2*A* shows a typical RP-HPLC elution profile of heterodimer produced from clone 19.7. The content of sIL-15Rα and IL-15 peaks were analyzed by SDS-PAGE (Fig. 2*B*) and the identities of both proteins were confirmed by immunoblot analysis (not shown). sIL-15Rα and IL-15 were eluted as broad peaks in several fractions), fractions 1–3 for IL-15Rα and fractions 4–13 for IL-15. Comparisons of the different fractions revealed small differences in size

among eluted proteins (Fig. 2), likely due to differences in post-translational modifications (*e.g.* glycosylation). To achieve >95% purity for sIL-15Rα, a pool of fractions 1–3 was subjected to chromatography on a 16 × 100-mm POROS R2/10 column (supplemental Fig. S2, *A* and *B*). IL-15 containing fractions 4–13 were also re-purified on the same column (supplemental Fig. S2, *C* and *D*). All purifications were performed under nonreducing conditions to maintain natural disulfide bonds in both proteins. The final pools of sIL-15Rα (supplemental Fig. S2, *A-B*, *Fx 1–3*) and IL-15 (supplemental Fig. S2, *C* and *D*, *Fx 2–5*) were analyzed by N-terminal Edman sequencing and the amount of each protein was determined by quantitative amino acid analysis. The molar ratio of the purified proteins recovered from the HPLC separation was ~1:1. sIL-15Rα and IL-15 were mixed at equivalent molar amounts in PBS, allowed to re-associate, then analyzed by native PAGE. Fig. 2*C* shows sIL-15Rα (*lane 1*), IL-15 (*lane 2*), and IL-15·sIL-15Rα complexes (*lane 3*) visualized by Coomassie Blue staining under nondenaturing conditions. No bands for the single chain IL-15 or sIL-15Rα were detectable in the lane where the IL-15·sIL-15Rα heterodimer was loaded (Fig. 2*C*, *lane 3*), indicating essentially quantitative formation of the IL-15·sIL-15Rα complex. Under native conditions, all three molecular species of sIL-15Rα, IL-15, and heterodimer were detected as diffuse bands, likely due to heterogeneity of glycosylation in human HEK293 cells.

Determination of C-terminal Sequence of sIL-15Rα—To determine the C-terminal sequence of naturally cleaved sIL-15Rα, purified sIL-15Rα (from clone 19.7) was digested with Lys-C endoproteinase, generating peptides suitable for N-terminal sequencing and mass spectrometry (MS) analyses. Truncated sIL-15Rα produced from clone 2.66 was also purified as described above for clone 19.7 and was used as reference because its C terminus sequence was known. The expected peptides after Lys-C endoproteinase digestion from truncated sIL-15Rα_2.66 are shown in supplemental Table S1. The peptides generated after Lys-C digestion from the naturally cleaved sIL-15Rα_19.7 were separated by RP-HPLC under nonreducing conditions, generating a smaller number of peptides for further analysis. The C-terminal peptide produced a broad peak that eluted early in RP-HPLC and was collected in several fractions (Fig. 3, *Fx 21–23*). Analysis by N-terminal protein sequencing of fraction 22 obtained after Lys-C proteolysis and RP-HPLC (Fig. 3) revealed 23 amino acid residues, *X*IRDPALVHQRPAPPS(T)V*XX*AGV, corresponding to residues 63–85 of the mature IL-15Rα (residues numbered according to the mature amino acid sequence) along with the 19-mer NWEL*X*A*X*ASHQPPGVYPQG, which corresponds to the sequence after Lys-151, the last Lys residue before the IL-15Rα transmembrane domain (supplemental Table S2). This suggested that $[M + H]^+$ of the C-terminal peptide should be at least 2038.962 (theoretical $[M + H]^+$ of peptide NWELTASASHQPPGVYPQG, which was identified by N-terminal sequencing). Analysis of fraction 22 by MALDI-TOF MS revealed the presence of several peptides with $[M + H]^+$ close to or greater than 2038.962 Da (Fig. 4). Upon protein sequence analysis of fraction 22 (NWEL*X*A*X*ASHQPPGVYPQG), we did not detect the expected Thr-5(in the protein:Thr-156) and Ser-7(in the protein:Ser-158), whereas we were able to detect Ser-9(in the protein:Ser-160). This suggested that Thr-5 and Ser-7 were most likely modified, probably through *O*-glycosylation. Analysis of *m*/*z* 2020.927, 2056.934, 2308.082, 2365.108, 2455.138, and 2770.224 in MS/MS mode showed very similar fragmentation spectra in the low mass region (up to 1225 Da), suggesting that these peptides were most likely derived from the same peptide sequence but present different post-translational modifications. The fragmentation spectra of *m*/*z* 2020.927, 2056.943, 2365.108, and 2770.224 and their analysis are shown in supplemental Fig. S4. Because *O*-glycosylation was likely to be on Thr-5 and Ser-7, the formation of unmodified N-terminal *b*-ions and C-terminal *y*-ions preceding these residues could be expected, potentially allowing the identification of the corre-

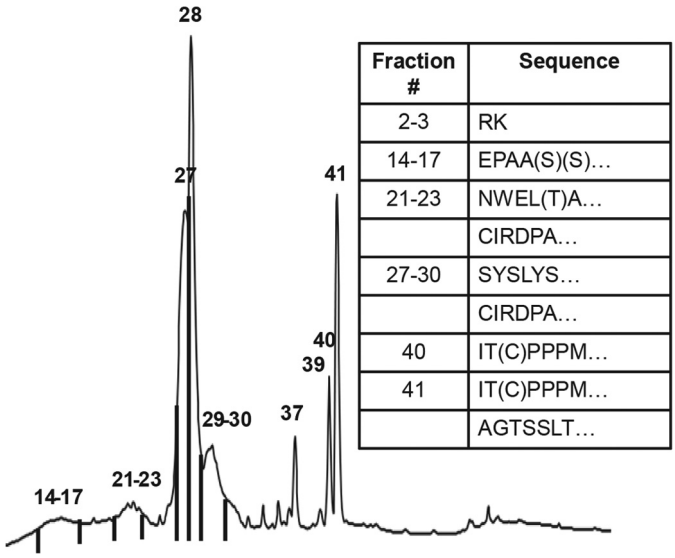

Fraction #	Sequence
2-3	RK
14-17	EPAA(S)(S)…
21-23	NWEL(T)A…
	CIRDPA…
27-30	SYSLYS…
	CIRDPA…
40	IT(C)PPPM…
41	IT(C)PPPM…
	AGTSSLT…

FIGURE 3. **HPLC separation of peptides after Lys-C digestion of purified naturally cleaved sIL-15Rα under nonreducing conditions.** sIL-15Rα from cell clone 19.7 was digested by Lys-C protease and peptides were separated by HPLC. Fractions were analyzed by a Applied Biosystems Inc. 477 A protein sequencer. The identified sequences shown in the *inset* were also confirmed by MALDI-TOF MS.

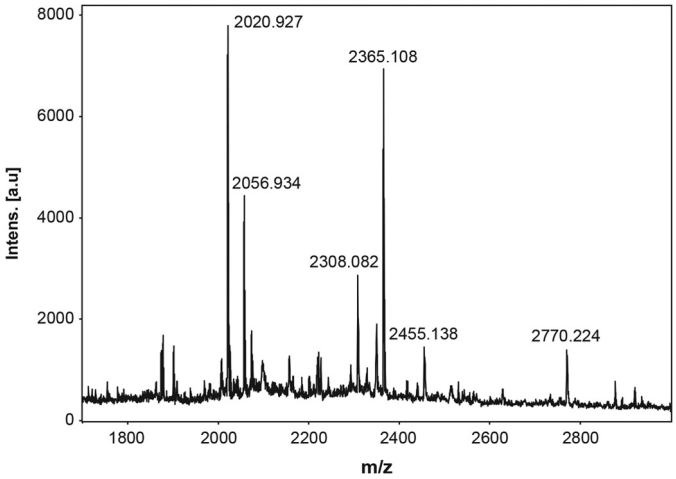

FIGURE 4. **MS analysis of HPLC fraction containing the C-terminal peptide of sIL15Rα.** MALDI-TOF MS revealed the presence of several peptides with *m*/*z* close (2020.927) or bigger (2056.934, 2308.082, 2365.108, 2455.138, and 2770.224) than expected for the peptide with sequence NWELTASASHQPPGVYPQG (theoretical $[M + H]^+$ 2038.962), which was determined by protein sequence analysis of this fraction.

sponding peptide using Mascot search of the protein sequence database. In all cases (*m*/*z* 2020.927, 2056.934, 2308.082, 2365.108, 2455.138, and 2770.224), the Mascot MS/MS ion search resulted in the identification of the same sequence of IL-15Rα that was obtained by protein sequencing, confirming that the NWELTASASHQPPGVYPQG sequence corresponds to the whole C-terminal peptide of naturally cleaved sIL-15Rα_19.7. A similar analysis was performed on naturally cleaved sIL-15Rα purified from clone 1.5, leading to the same conclusion. Taken together, these data demonstrate that the proteolytic cleavage of membrane-bound IL-15Rα takes place between Gly-170 and His-171 in two different cell clones. Truncated engineered sIL-15Rα produced from clone 2.66 includes 5 additional amino acids at the C terminus (Fig. 1).

Identification of Post-translational Modifications of sIL-15Rα—Analysis of the naturally cleaved sIL-15Rα expressed from stable human cell lines by MALDI-TOF MS revealed the presence of numerous post-translational modifications. The expected molecular mass of the polypeptide chain of sIL-15Rα (170 amino acids) is 17,839.86 Da (Fig. 1). MALDI-TOF MS analysis of the purified sIL-15Rα revealed a broad peak with a center at 34,910 Da (supplemental Fig. S3), implying that almost half of its molecular mass is due to post-translational modifications, most likely *O*- and *N*-linked glycosylation. Detailed analysis characterized the post-translational modification in the C- and N-terminal region of naturally cleaved sIL-15Rα. The C-terminal peptide with *m*/*z* 2020.927 (Fig. 4) was 18 Da less than the predicted NWELTASASHQPPGVYPQG peptide with *m*/*z* 2038.962, indicating loss of water. Because *O*-glycosylations were the likely modifications in the C-terminal region of sIL-15Rα, it is possible that 2020.927 is the product of the β-elimination reaction during proteolysis of the purified sIL-15Rα by Lys-C digestion. A β-elimination reaction at *O*-glycosylated Ser and Thr residues would lead to loss of water with formation of dehydroalanine and dehydroaminobutyric acid, correspondingly. Peptides with dehydroamino acid residues containing a reactive double bond are not stable and quickly react with available nucleophilic compounds. The peptide with *m*/*z* 2020.927 appeared to be stable and did not react with 2-aminoethanethiol suggesting that its double bond probably reacted intramolecularly with the hydroxyl group of a neighboring Ser or Thr residue. The ion fragment spectrum of parent ion 2020.927 is shown in supplemental Fig. S4*A*. The peptide with *m*/*z* 2056.934 differs from 2020.927 by 36 Da and represented the *m*/*z* of the same NWELTASASHQPPGVYPQG peptide, which first lost water due to β-elimination and then added HCl to the double bond of a dehydroamino acid. The ion fragment spectrum of parent ion 2056.934 is shown in supplemental Fig. S4*B*. Analysis of this spectrum in BioTools with modification (chlorine addition) on Thr-5 and Ser-7 suggested that *O*-glycosylation took place at these sites with equal probability. Analysis of ion fragment spectra of parent ions 2308.082, 2365.108, 2455.138, and 2770.224 suggested that they have *O*-linked oligosaccharides attached to the peptide with *m*/*z* 2038.962 (supplemental Fig. S4, *C* and *D*).

We also performed a detailed characterization of the N-terminal region of sIL-15Rα. MALDI-TOF MS/MS of *m*/*z* 1922.963 (Fig. 3; fraction 40) identified the N-terminal peptide ITCPPPMSVEHADIWVK of sIL-15Rα. However, *m*/*z* 2126.150 of fraction 39 gave a similar fragment ion spectrum, suggesting that both ions correspond to the same peptide. Mascot MS/MS ion search using fragment ions derived from 2126.150 when the parent ion was set as 1922.950 (corresponding to the theoretical *m*/*z* of unmodified peptide) confidently identified the same sequence ITCPPPMSVEHADIWVK (supplemental Fig. S5*A*). The mass difference between these *m*/*z* is 203.187, which is close to the mass of *N*-acetylhexosamine (HexNAc; *N*-acetylgalactosamine or *N*-acetylglucosamine). Analysis of the spectra with the modification set on Ser-8 (supplemental Fig. S5*B*) and Thr-2 (supplemental Fig. S5*C*) suggested that the modified residue was most likely Ser-8 because no additional expected modified *b*-ions were detected when modification was set on Thr-2. There are several Ser residues in the N-terminal sequence of IL-15Rα beyond Ser-8. To determine whether some of these residues are also modified, purified sIL-15Rα was analyzed by In-Source Decay MALDI-TOF MS. The spectrum was analyzed using Top-Down Mascot Search of the Sprot human database, which allowed the identification of the mature N-terminal sequence of IL-15Rα (supplemental Fig. S6*A*). Analysis of the spectrum confirmed that Ser-8 is partially modified by *N*-acetylhexosamine (HexNAc) along with Ser-18, -20, -23, and -31 (supplemental Fig. S6, *B*-*F*). These data showed that naturally cleaved sIL-15Rα produced from human cells is heavily glycosylated with *N*- and *O*-linked glycosylation both in the N- and C-terminal regions of the protein (Fig. 1).

Determination of in Vivo Half-life of Different Forms of IL-15—IL-15·sIL-15Rα heterodimer produced from human cell lines retains all the naturally occurring post-translational modifications, such as native disulfide bonds and both *N*- and *O*-linked glycosylation (Fig. 1). These post-translational modifications are absent in *E. coli*-derived monomeric IL-15 (29) and, along with the lack of the IL-15Rα subunit, could affect the stability, pharmacokinetics, and bioactivity of IL-15 cytokine.

The purified IL-15 and sIL-15Rα chains were reconstituted as described above (Fig. 2*C*) and used in experiments *in vivo* to evaluate their pharmacokinetic and pharmacodynamic properties in comparison to both single chain nonglycosylated IL-15 produced in *E. coli* and purified by conventional chromatography (29) and glycosylated single chain IL-15 produced by human HEK293 cells and purified as described above (Fig. 2). To evaluate the *in vivo* half-life of IL-15·sIL-15Rα heterodimers in comparison to single chain IL-15, mice (5/group) were injected intraperitoneally with 3 μg of human *E. coli*-derived single chain IL-15, 3 μg of human HEK293 cell-derived single chain IL-15, or an equimolar amount of purified human IL-15·sIL-15Rα (corresponding to 3 μg of IL-15 monomer, clone 1.5 lot 1). Serum was collected at various times after injection and IL-15 levels were measured by ELISA (Fig. 5). Both single chain IL-15 preparations reached peak plasma levels at 30 min after protein administration (~70 and ~25 ng/ml for *E. coli*-derived and human HEK293 cell-derived IL-15, respectively). The difference in the IL-15 plasma levels between these two preparations is most likely a consequence of the different capability of the ELISA antibodies to detect unglycosylated and

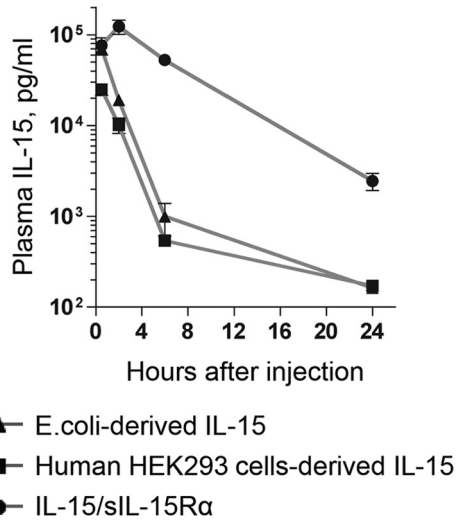

FIGURE 5. **Association with sIL-15Ra increases the *in vivo* half-life of human IL-15 in mice.** Five mice per group were injected with equimolar quantities of *E. coli* single chain IL-15, human HEK293 cell-derived single chain IL-15, or IL-15·sIL-15Rα heterodimer (3 μg IL-15 eq/mice, intraperitoneally). The mice were bled over time (0.5, 2, 6, and 24 h after treatment), plasma IL-15 levels were evaluated by ELISA, and reported as mean ± S.D.

glycosylated IL-15 (data not shown). In contrast, administration of the IL-15·sIL-15Rα heterodimer resulted in higher peak IL-15 levels 2 h after injection (~120 ng/ml). The half-life of both single chain IL-15 preparations was similar and less than 30 min, whereas the IL-15·sIL-15Rα heterodimer had a significantly extended half-life (~4 h) (Fig. 5). The area under the curve for the 24-h period was 20 times higher for the heterodimer, compared with both single chain IL-15. Similar results were obtained after intravenous or subcutaneous administration (data not shown). Human cell-produced IL-15·sIL-15Rα heterodimer thus has a favorable pharmacokinetic profile in mice in comparison to single chain IL-15.

Bioactivity of Heterodimeric IL-15·sIL-15Rα in Vivo—We also compared the biological activity of the different forms of IL-15 in mice. CFSE-labeled splenocytes were transferred into C57BL/6 mice. The mice were subsequently treated with PBS, with 3 μg of *E. coli*-derived single chain IL-15, or with an equimolar amount of IL-15·sIL-15Rα. Proliferation of transferred cells was evaluated 4 days after treatment. IL-15·sIL-15Rα heterodimer induced a greater proliferation of donor $CD8^+$ T cells (Fig. 6*A*, *top panels*) and NK cells (Fig. 6*A*, *bottom panels*) in comparison to single chain IL-15 with a higher frequency of proliferating cells, and more rounds of cell division. Upon single chain IL-15 injection, few $CD8^+$ T cells divided even once, whereas the IL-15·sIL-15Rα heterodimer induced multiple rounds of division, resulting in a significant increase in the frequency of $CD8^+$ T cells in spleen. Thus, the IL-15·sIL-15Rα heterodimer was more stable *in vivo*, had a prolonged serum half-life, and was more bioactive on a molar basis, compared with single chain IL-15. The serum levels of IL-15 correlated with the biological activity, as measured by CFSE dilution of transferred cells (Fig. 6*A*). Although the overall proliferation of $CD4^+$ T cells did not change upon IL-15 administration, analysis of different subsets of memory $CD4^+$ T cells showed an expansion of effector memory cells (data not shown), as previously reported (32–34). We also confirmed the increased proliferation of $CD8^+$ T and NK cells upon IL-15 administration by measuring the frequency of cells expressing Ki-67. Mice (5/group) were injected intraperitoneally with 3 μg of human *E. coli*-derived single chain IL-15, 3 μg of human HEK293 cell-derived single chain IL-15, or an equimolar amount of purified human IL-15·sIL-15Rα. At day 4 after protein administration, all IL-15-treated mice showed an increased frequency of Ki-67^+ $CD8^+$ T and NK cells in comparison to PBS-treated mice (Fig. 6*B*). IL-15 heterodimer induced a greater proliferation of these lymphocyte subsets in comparison to both single chain IL-15 preparations, which were characterized by a similar bioactivity in agreement with their similar pharmacokinetic profile.

The bioactivity of IL-15 heterodimer formulations was similar in different purified lots. Mice were injected intraperitoneally with 3 μg of human IL-15·sIL-15Rα from two separate purification lots and sacrificed at day 3 after injection (Fig. 6*C*). Administration of human IL-15·sIL-15Rα in mice resulted in an increased frequency of proliferating $CD8^+$ T cells (defined as Ki-67^+) in comparison to untreated mice after both intraperitoneal (Fig. 6*C*) and intravenous delivery (data not shown). No difference in bioactivity (measured as $CD8^+$ T cell proliferation) was observed comparing IL-15·sIL-15Rα obtained from different production/purification lots (Fig. 6*C*).

DISCUSSION

IL-15 is a important cytokine with potential clinical applications as a lymphocyte growth and activation factor (15). Recombinant human IL-15 generated in *E. coli* has been produced as a nonglycosylated monomer of ~12 kDa (29). Preclinical studies to evaluate safety, toxicity, pharmacokinetics, and pharmacodynamics of monomeric human IL-15 have been conducted in rhesus macaques, and showed an increase in the absolute number and proliferation of NK and $CD8^+$ T cells (33–36). Although monomeric *E. coli*-produced IL-15 is in the initial stages of clinical testing, this form of the molecule poses multiple challenges for clinical use due to its instability and rapid plasma clearance (35, 36). IL-15 expression is tightly regulated at the transcriptional level, as well as at several post-transcriptional and post-translational steps such as mRNA stability, generation of alternative spliced isoforms, intracellular trafficking, interaction with IL-15Rα, and secretion (21, 22, 24, 37–42). We have employed a systematic approach to reproduce in engineered human cells the natural steps of production and processing of IL-15·sIL-15Rα heterodimers, resulting in efficient production and purification of the bioactive IL-15 heterodimeric cytokine, which appears to have important potential advantages over the monomeric form of the molecule. Taking advantage of the stabilization of IL-15 by co-expression with IL-15Rα (22), we produced combination vectors expressing the heterodimeric cytokine IL-15·IL-15Rα, providing strong improvements in yield (21, 22). These vectors were used to develop stable clonal human HEK293 cells that grow in serum-free medium and express and secrete high levels of human IL-15·sIL-15Rα complexes (up to 70 mg of IL-15/liter). We developed an efficient procedure for the purification of biologically active IL-15·sIL-15Rα heterodimers based on nonre-

ducing RP-HPLC. The IL-15 and sIL-15Rα chains of the IL-15 heterodimeric cytokine are noncovalently linked and can be separated under certain conditions, such as pH < 3.5 (16). This allowed us to produce pure preparations of single chain IL-15 and sIL-15Rα. Importantly, RP-HPLC was performed under nonreducing conditions, avoiding the need for protein refolding after purification. Because the K_d of the two chains is $\sim 10^{-11}$ M (30, 43), the purified IL-15 and sIL-15Rα subunits can be combined *in vitro* in a 1:1 molar ratio in PBS allowing rapid formation of the bioactive heterodimeric cytokine. IL-15

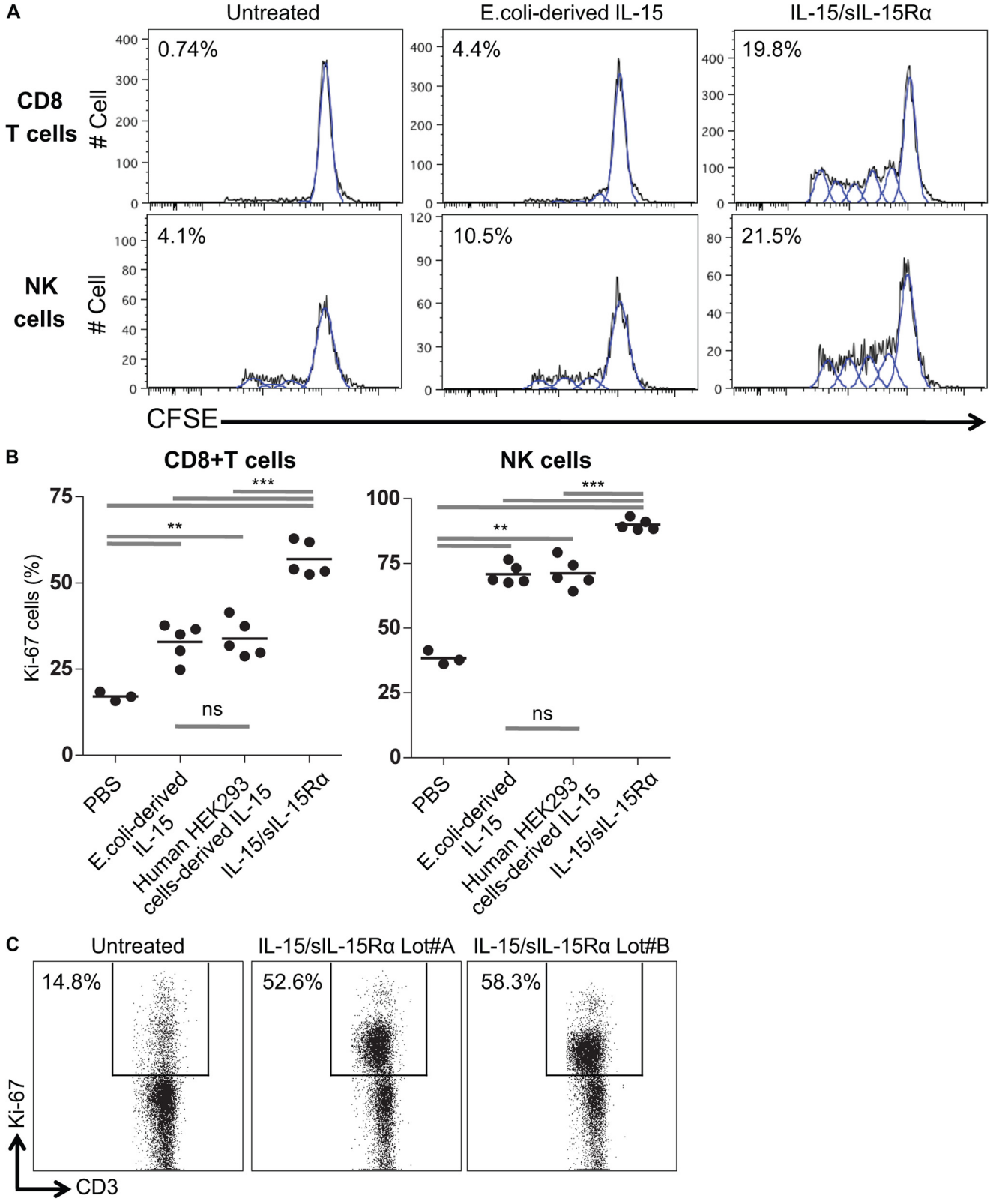

is stabilized in the presence of IL-15Rα, and the generation of IL-15 as a heterodimeric cytokine has the additional benefit to be a more stable structure, avoiding denaturation and inactivation and decreasing the possibility of creating immunogenic forms.

HEK293 human cells produce correctly folded, processed, and glycosylated human IL-15·sIL-15Rα heterodimeric cytokine. Both IL-15 and sIL-15Rα subunits of the heterodimeric cytokine contain intramolecular disulfide bonds and are heavily glycosylated (Fig. 1). IL-15 has three potential *N*-linked glycosylation sites (44). In agreement with a previous publication (31), the data presented in this study show that sIL-15Ra contains both *N*- and *O*-linked carbohydrates both in the N- and C-portion of the molecule. Several studies have demonstrated the contribution of glycosylation to the effect of cytokines and growth factors (for reviews, see Refs. 45 and 46). Glycosylated interferon-β (47), erythropoietin (48, 49), granulocyte colony stimulating factor (50), and IL-7 (51) are more stable and bioactive in comparison to the nonglycosylated forms. Glycosylation was also reported to affect the interaction with specific receptors, as IL-7 was able to bind glycosylated IL-7Rα 300-fold more tightly than unglycosylated IL-7Rα (52). Additionally, production of factors for clinical use in human cells may reduce the risk of immunogenicity. Administration of recombinant human granulocyte macrophage colony stimulating factor was associated with the development of antibodies against the recombinant protein. These antibodies were found to react against sites on the protein that are normally protected by *O*-linked carbohydrates (49). Similarly, administration of *E. coli*-derived human IL-7 in humans induced antibodies against the recombinant protein (53), whereas no anti-IL-7 antibodies were found using the glycosylated cytokine (CYT107) (54). Immunogenicity of *E. coli*-derived single chain human IL-15 has been reported in macaques where the development of anti-IL-15 antibodies was observed upon subcutaneous administration (35).

Pharmacokinetic and pharmacodynamic properties of the purified glycosylated human IL-15 heterodimers were investigated in mice. In comparison to single chain IL-15 produced both in *E. coli* and in human HEK293 cells, IL-15·sIL-15Rα complexes showed a more prolonged serum half-life and were more bioactive on a molar basis. The superior bioactivity of IL-15 in the heterodimeric formulation is mainly the result of the presence of IL-15Rα contributing to increased stability of the protein *in vivo*. These properties offer the potential to allow lower and less frequent dosing and simpler delivery methods, with increased convenience for both patients and caregivers. The crystal structures of the heterodimer IL-15·IL-15Ra and the quaternary IL-15·IL-15Rα·IL-2Rβ-γc complex have been reported (55, 56). These reports identify the amino acids and domains involved in the binding between chains. Importantly, IL-15 has two distinct binding sites, site I for the binding to IL-2Rβ and site II for the binding to IL-2Rγc. In contrast, IL-15Rα does not contact IL-2Rβ, with a distance of >15 Å separating the subunits at their closest point. It is also reported that the IL-15·IL-15Rα heterodimer binds to IL-2Rβ with an affinity ~150-fold greater than that of single chain IL-15, suggesting that IL-15 stabilization is a major function of IL-15Rα (56).

The production and purification of IL-15 associated with the sushi domain of IL-15Rα linked to the Fc region of IgG1 has been previously reported (57). This molecule was also reported to show favorable pharmacokinetics and increased biological activity in comparison to single chain IL-15 both *in vitro* and *in vivo*. However, the authentically processed and glycosylated IL-15·sIL-15Rα, as produced and purified in this study, has the advantage to be the closest to the IL-15 produced in the human body and circulating in plasma (23) and may be the least immunogenic form.

The availability of naturally cleaved purified sIL-15Rα has allowed us to investigate processing and shedding of IL-15Rα from the cell surface. MALDI-TOF MS analysis, protein sequencing, and Mascot searches of protein sequence databases confidently identified the proteolytic cleavage site of membrane-bound IL-15Rα between Gly-170 and His-171 of the mature membrane-associated form of IL-15Rα (Fig. 1). The determination of the sequence corresponding to the cleavage site in IL-15Rα and the amino acid sequence of the mature sIL-15Rα represent an important finding in support of further studies, aiming to identify how this process is regulated. Dysregulated shedding of IL-15·IL-15Rα heterodimers from the cell surface may be one mechanism leading to the altered levels of circulating IL-15 upon certain conditions, *i.e.* lymphodepleting treatments (23, 26) and autoimmune diseases, such as celiac disease (58), rheumatoid arthritis (59), and multiple sclerosis (60). Dissecting the molecular mechanism and regulation of the IL-15·IL-15Rα shedding process may offer opportunities for therapeutic targeting in IL-15-associated pathological conditions and may help the design of better therapeutic and/or prognostic strategies.

In summary, our study demonstrates that high-level production of authentically processed and glycosylated human IL-15·sIL-15Rα heterodimers is achievable in human cells and that RP-HPLC under nonreducing conditions allows the purification of biologically active heterodimers, avoiding protein refolding. Purified glycosylated IL-15 heterodimers have the

FIGURE 6. **IL-15·sIL-15Ra heterodimer is bioactive *in vivo*.** *A,* IL-15·sIL-15Rα heterodimer is more potent than single chain IL-15, *in vivo* lymphocyte proliferation. 12 h after transfer of CFSE-labeled splenocytes (20×10^6), mice were treated intraperitoneally with PBS (3 mice), with 3 μg of IL-15 (3 mice), or with equimolar quantity of IL-15·sIL-15Rα (3 mice, 3 μg in single chain IL-15). $CD8^+$ T cells (top panels) and NK cells (*bottom panels*) were analyzed on day 4 by flow cytometry for CFSE fluorescence. One representative mouse per group is shown. *B,* IL-15Rα contributes to the superior activity of IL-15 heterodimers. Mice were treated intraperitoneally with PBS (3 mice), with 3 μg of *E. coli*-derived single chain IL-15 (5 mice), with 3 μg of human HEK293 cell-derived single chain IL-15 (5 mice), or with an equimolar quantity of IL-15·sIL-15Rα (5 mice, 3 μg in single chain IL-15). The frequency of $CD8^+$ T cells (*left panels*) and NK cells (*right panel*) expressing the proliferative marker Ki-67 is shown. Individual animals and average are shown for each group. **, $p < 0.01$; ***, $p < 0.001$; *ns*, nonsignificant. *C,* different lots of purified IL-15·sIL-15Rα heterodimer from clone 1.5 induced similar levels of proliferation in splenic $CD8^+$ T cells. Mice were treated intraperitoneally with PBS or with 3 μg of IL-15·sIL-15Rα (clone 1.5 lot A) or 3 μg of IL-15·sIL-15Rα (clone 1.5 lot B). Isolated splenocytes were evaluated on day 3 by flow cytometry for the presence of the proliferation marker Ki-67. Percentage of Ki-67^+ cells within the $CD8^+$ T cell population is shown. One representative mouse per group (3 mice/group) is shown.

advantage of increased stability and bioactivity *in vivo* and warrant evaluation in clinical studies.

Acknowledgments—We thank A. Valentin, M. Rosati, C. Alicea, and J. J. S. Cadwell for critical discussions and technical assistance, and T. Jones for editorial assistance.

REFERENCES

1. Berard, M., Brandt, K., Bulfone-Paus, S., and Tough, D. F. (2003) IL-15 promotes the survival of naive and memory phenotype $CD8^+$ T cells. *J. Immunol.* **170,** 5018–5026
2. Carson, W. E., Giri, J. G., Lindemann, M. J., Linett, M. L., Ahdieh, M., Paxton, R., Anderson, D., Eisenmann, J., Grabstein, K., and Caligiuri, M. A. (1994) Interleukin (IL) 15 is a novel cytokine that activates human natural killer cells via components of the IL-2 receptor. *J. Exp. Med.* **180,** 1395–1403
3. Ma, A., Koka, R., and Burkett, P. (2006) Diverse functions of IL-2, IL-15, and IL-7 in lymphoid homeostasis. *Annu. Rev. Immunol.* **24,** 657–679
4. Tan, J. T., Ernst, B., Kieper, W. C., LeRoy, E., Sprent, J., and Surh, C. D. (2002) Interleukin (IL)-15 and IL-7 jointly regulate homeostatic proliferation of memory phenotype $CD8^+$ cells but are not required for memory phenotype $CD4^+$ cells. *J. Exp. Med.* **195,** 1523–1532
5. Zhang, X., Sun, S., Hwang, I., Tough, D. F., and Sprent, J. (1998) Potent and selective stimulation of memory-phenotype $CD8^+$ T cells *in vivo* by IL-15. *Immunity* **8,** 591–599
6. Dubois, S., Patel, H. J., Zhang, M., Waldmann, T. A., and Müller, J. R. (2008) Preassociation of IL-15 with IL-15R α-IgG1-Fc enhances its activity on proliferation of NK and $CD8^+$/CD44 high T cells and its antitumor action. *J. Immunol.* **180,** 2099–2106
7. Epardaud, M., Elpek, K. G., Rubinstein, M. P., Yonekura, A. R., Bellemare-Pelletier, A., Bronson, R., Hamerman, J. A., Goldrath, A. W., and Turley, S. J. (2008) Interleukin-15/interleukin-15R α complexes promote destruction of established tumors by reviving tumor-resident $CD8^+$ T cells. *Cancer Res.* **68,** 2972–2983
8. Klebanoff, C. A., Finkelstein, S. E., Surman, D. R., Lichtman, M. K., Gattinoni, L., Theoret, M. R., Grewal, N., Spiess, P. J., Antony, P. A., Palmer, D. C., Tagaya, Y., Rosenberg, S. A., Waldmann, T. A., and Restifo, N. P. (2004) IL-15 enhances the *in vivo* antitumor activity of tumor-reactive $CD8^+$ T cells. *Proc. Natl. Acad. Sci. U.S.A.* **101,** 1969–1974
9. Kobayashi, H., Dubois, S., Sato, N., Sabzevari, H., Sakai, Y., Waldmann, T. A., and Tagaya, Y. (2005) Role of trans-cellular IL-15 presentation in the activation of NK cell-mediated killing, which leads to enhanced tumor immunosurveillance. *Blood* **105,** 721–727
10. Stoklasek, T. A., Schluns, K. S., and Lefrançois, L. (2006) Combined IL-15/IL-15Rα immunotherapy maximizes IL-15 activity *in vivo*. *J. Immunol.* **177,** 6072–6080
11. Teague, R. M., Sather, B. D., Sacks, J. A., Huang, M. Z., Dossett, M. L., Morimoto, J., Tan, X., Sutton, S. E., Cooke, M. P., Ohlén, C., and Greenberg, P. D. (2006) Interleukin-15 rescues tolerant $CD8^+$ T cells for use in adoptive immunotherapy of established tumors. *Nat. Med.* **12,** 335–341
12. Zhang, M., Yao, Z., Dubois, S., Ju, W., Müller, J. R., and Waldmann, T. A. (2009) Interleukin-15 combined with an anti-CD40 antibody provides enhanced therapeutic efficacy for murine models of colon cancer. *Proc. Natl. Acad. Sci. U.S.A.* **106,** 7513–7518
13. Cheever, M. A. (2008) Twelve immunotherapy drugs that could cure cancers. *Immunol. Rev.* **222,** 357–368
14. Croce, M., Orengo, A. M., Azzarone, B., and Ferrini, S. (2012) Immunotherapeutic applications of IL-15. *Immunotherapy* **4,** 957–969
15. Waldmann, T. A. (2006) The biology of interleukin-2 and interleukin-15. Implications for cancer therapy and vaccine design. *Nat. Rev. Immunol.* **6,** 595–601
16. Dubois, S., Mariner, J., Waldmann, T. A., and Tagaya, Y. (2002) IL-15Rα recycles and presents IL-15 in *trans* to neighboring cells. *Immunity* **17,** 537–547
17. Burkett, P. R., Koka, R., Chien, M., Chai, S., Boone, D. L., and Ma, A. (2004) Coordinate expression and trans presentation of interleukin (IL)-15Rα and IL-15 supports natural killer cell and memory $CD8^+$ T cell homeostasis. *J. Exp. Med.* **200,** 825–834
18. Koka, R., Burkett, P. R., Chien, M., Chai, S., Chan, F., Lodolce, J. P., Boone, D. L., and Ma, A. (2003) Interleukin (IL)-15Rα-deficient natural killer cells survive in normal but not IL-15Rα-deficient mice. *J. Exp. Med.* **197,** 977–984
19. Sandau, M. M., Schluns, K. S., Lefrancois, L., and Jameson, S. C. (2004) Cutting edge. Transpresentation of IL-15 by bone marrow-derived cells necessitates expression of IL-15 and IL-15Rα by the same cells. *J. Immunol.* **173,** 6537–6541
20. Schluns, K. S., Kieper, W. C., Jameson, S. C., and Lefrançois, L. (2000) Interleukin-7 mediates the homeostasis of naive and memory CD8 T cells *in vivo*. *Nat. Immunol.* **1,** 426–432
21. Bergamaschi, C., Jalah, R., Kulkarni, V., Rosati, M., Zhang, G. M., Alicea, C., Zolotukhin, A. S., Felber, B. K., and Pavlakis, G. N. (2009) Secretion and biological activity of short signal peptide IL-15 is chaperoned by IL-15 receptor α *in vivo*. *J. Immunol.* **183,** 3064–3072
22. Bergamaschi, C., Rosati, M., Jalah, R., Valentin, A., Kulkarni, V., Alicea, C., Zhang, G. M., Patel, V., Felber, B. K., and Pavlakis, G. N. (2008) Intracellular interaction of interleukin-15 with its receptor α during production leads to mutual stabilization and increased bioactivity. *J. Biol. Chem.* **283,** 4189–4199
23. Bergamaschi, C., Bear, J., Rosati, M., Beach, R. K., Alicea, C., Sowder, R., Chertova, E., Rosenberg, S. A., Felber, B. K., and Pavlakis, G. N. (2012) Circulating IL-15 exists as heterodimeric complex with soluble IL-15Rα in human and mouse serum. *Blood* **120,** e1–8
24. Mortier, E., Woo, T., Advincula, R., Gozalo, S., and Ma, A. (2008) IL-15Rα chaperones IL-15 to stable dendritic cell membrane complexes that activate NK cells via trans presentation. *J. Exp. Med.* **205,** 1213–1225
25. Rubinstein, M. P., Kadima, A. N., Salem, M. L., Nguyen, C. L., Gillanders, W. E., and Cole, D. J. (2002) Systemic administration of IL-15 augments the antigen-specific primary $CD8^+$ T cell response following vaccination with peptide-pulsed dendritic cells. *J. Immunol.* **169,** 4928–4935
26. Dudley, M. E., Yang, J. C., Sherry, R., Hughes, M. S., Royal, R., Kammula, U., Robbins, P. F., Huang, J., Citrin, D. E., Leitman, S. F., Wunderlich, J., Restifo, N. P., Thomasian, A., Downey, S. G., Smith, F. O., Klapper, J., Morton, K., Laurencot, C., White, D. E., and Rosenberg, S. A. (2008) Adoptive cell therapy for patients with metastatic melanoma: evaluation of intensive myeloablative chemoradiation preparative regimens. *J. Clin. Oncol.* **26,** 5233–5239
27. Jalah, R., Rosati, M., Kulkarni, V., Patel, V., Bergamaschi, C., Valentin, A., Zhang, G. M., Sidhu, M. K., Eldridge, J. H., Weiner, D. B., Pavlakis, G. N., and Felber, B. K. (2007) Efficient systemic expression of bioactive IL-15 in mice upon delivery of optimized DNA expression plasmids. *DNA Cell Biol.* **26,** 827–840
28. Mortier, E., Bernard, J., Plet, A., and Jacques, Y. (2004) Natural, proteolytic release of a soluble form of human IL-15 receptor α-chain that behaves as a specific, high affinity IL-15 antagonist. *J. Immunol.* **173,** 1681–1688
29. Vyas, V. V., Esposito, D., Sumpter, T. L., Broadt, T. L., Hartley, J., Knapp, G. C., 4th, Cheng, W., Jiang, M. S., Roach, J. M., Yang, X., Giardina, S. L., Mitra, G., Yovandich, J. L., Creekmore, S. P., Waldmann, T. A., and Zhu, J. (2012) Clinical manufacturing of recombinant human interleukin 15. I. Production cell line development and protein expression in *E. coli* with stop codon optimization. *Biotechnol. Prog.* **28,** 497–507
30. Anderson, D. M., Kumaki, S., Ahdieh, M., Bertles, J., Tometsko, M., Loomis, A., Giri, J., Copeland, N. G., Gilbert, D. J., and Jenkins, N. A. (1995) Functional characterization of the human interleukin-15 receptor α chain and close linkage of IL15RA and IL2RA genes. *J. Biol. Chem.* **270,** 29862–29869
31. Dubois, S., Magrangeas, F., Lehours, P., Raher, S., Bernard, J., Boisteau, O., Leroy, S., Minvielle, S., Godard, A., and Jacques, Y. (1999) Natural splicing of exon 2 of human interleukin-15 receptor α-chain mRNA results in a shortened form with a distinct pattern of expression. *J. Biol. Chem.* **274,** 26978–26984
32. Picker, L. J., Reed-Inderbitzin, E. F., Hagen, S. I., Edgar, J. B., Hansen, S. G., Legasse, A., Planer, S., Piatak, M., Jr., Lifson, J. D., Maino, V. C., Axthelm, M. K., and Villinger, F. (2006) IL-15 induces CD4 effector memory T cell production and tissue emigration in nonhuman primates. *J. Clin. Invest.*

116, 1514–1524
33. Berger, C., Berger, M., Hackman, R. C., Gough, M., Elliott, C., Jensen, M. C., and Riddell, S. R. (2009) Safety and immunologic effects of IL-15 administration in nonhuman primates. *Blood* **114,** 2417–2426
34. Lugli, E., Goldman, C. K., Perera, L. P., Smedley, J., Pung, R., Yovandich, J. L., Creekmore, S. P., Waldmann, T. A., and Roederer, M. (2010) Transient and persistent effects of IL-15 on lymphocyte homeostasis in nonhuman primates. *Blood* **116,** 3238–3248
35. Sneller, M. C., Kopp, W. C., Engelke, K. J., Yovandich, J. L., Creekmore, S. P., Waldmann, T. A., and Lane, H. C. (2011) IL-15 administered by continuous infusion to rhesus macaques induces massive expansion of $CD8^+$ T effector memory population in peripheral blood. *Blood* **118,** 6845–6848
36. Waldmann, T. A., Lugli, E., Roederer, M., Perera, L. P., Smedley, J. V., Macallister, R. P., Goldman, C. K., Bryant, B. R., Decker, J. M., Fleisher, T. A., Lane, H. C., Sneller, M. C., Kurlander, R. J., Kleiner, D. E., Pletcher, J. M., Figg, W. D., Yovandich, J. L., and Creekmore, S. P. (2011) Safety (toxicity), pharmacokinetics, immunogenicity, and impact on elements of the normal immune system of recombinant human IL-15 in rhesus macaques. *Blood* **117,** 4787–4795
37. Bamford, R. N., DeFilippis, A. P., Azimi, N., Kurys, G., and Waldmann, T. A. (1998) The 5′ untranslated region, signal peptide, and the coding sequence of the carboxyl terminus of IL-15 participate in its multifaceted translational control. *J. Immunol.* **160,** 4418–4426
38. Onu, A., Pohl, T., Krause, H., and Bulfone-Paus, S. (1997) Regulation of IL-15 secretion via the leader peptide of two IL-15 isoforms. *J. Immunol.* **158,** 255–262
39. Tagaya, Y., Bamford, R. N., DeFilippis, A. P., and Waldmann, T. A. (1996) IL-15. A pleiotropic cytokine with diverse receptor/signaling pathways whose expression is controlled at multiple levels. *Immunity* **4,** 329–336
40. Tagaya, Y., Kurys, G., Thies, T. A., Losi, J. M., Azimi, N., Hanover, J. A., Bamford, R. N., and Waldmann, T. A. (1997) Generation of secretable and nonsecretable interleukin 15 isoforms through alternate usage of signal peptides. *Proc. Natl. Acad. Sci. U.S.A.* **94,** 14444–14449
41. Waldmann, T. A., and Tagaya, Y. (1999) The multifaceted regulation of interleukin-15 expression and the role of this cytokine in NK cell differentiation and host response to intracellular pathogens. *Annu. Rev. Immunol.* **17,** 19–49
42. Duitman, E. H., Orinska, Z., Bulanova, E., Paus, R., and Bulfone-Paus, S. (2008) How a cytokine is chaperoned through the secretory pathway by complexing with its own receptor. Lessons from interleukin-15 (IL-15)/IL-15 receptor α. *Mol. Cell. Biol.* **28,** 4851–4861
43. Giri, J. G., Kumaki, S., Ahdieh, M., Friend, D. J., Loomis, A., Shanebeck, K., DuBose, R., Cosman, D., Park, L. S., and Anderson, D. M. (1995) Identification and cloning of a novel IL-15 binding protein that is structurally related to the α chain of the IL-2 receptor. *EMBO J.* **14,** 3654–3663
44. Kurys, G., Tagaya, Y., Bamford, R., Hanover, J. A., and Waldmann, T. A. (2000) The long signal peptide isoform and its alternative processing direct the intracellular trafficking of interleukin-15. *J. Biol. Chem.* **275,** 30653–30659
45. Solá, R. J., and Griebenow, K. (2009) Effects of glycosylation on the stability of protein pharmaceuticals. *J. Pharm. Sci.* **98,** 1223–1245
46. Chamorey, A. L., Magné, N., Pivot, X., and Milano, G. (2002) Impact of glycosylation on the effect of cytokines. A special focus on oncology. *Eur. Cytokine Netw.* **13,** 154–160
47. Karpusas, M., Whitty, A., Runkel, L., and Hochman, P. (1998) The structure of human interferon-β. Implications for activity. *Cell Mol. Life Sci.* **54,** 1203–1216
48. Takeuchi, M., and Kobata, A. (1991) Structures and functional roles of the sugar chains of human erythropoietins. *Glycobiology* **1,** 337–346
49. Gribben, J. G., Devereux, S., Thomas, N. S., Keim, M., Jones, H. M., Goldstone, A. H., and Linch, D. C. (1990) Development of antibodies to unprotected glycosylation sites on recombinant human GM-CSF. *Lancet* **335,** 434–437
50. Querol, S., Cancelas, J. A., Amat, L., Capmany, G., and Garcia, J. (1999) Effect of glycosylation of recombinant human granulocytic colony-stimulating factor on expansion cultures of umbilical cord blood $CD34^+$ cells. *Haematologica* **84,** 493–498
51. Beq, S., Rozlan, S., Gautier, D., Parker, R., Mersseman, V., Schilte, C., Assouline, B., Rancé, I., Lavedan, P., Morre, M., and Cheynier, R. (2009) Injection of glycosylated recombinant simian IL-7 provokes rapid and massive T-cell homing in rhesus macaques. *Blood* **114,** 816–825
52. McElroy, C. A., Dohm, J. A., and Walsh, S. T. (2009) Structural and biophysical studies of the human IL-7/IL-7Rα complex. *Structure* **17,** 54–65
53. Rosenberg, S. A., Sportès, C., Ahmadzadeh, M., Fry, T. J., Ngo, L. T., Schwarz, S. L., Stetler-Stevenson, M., Morton, K. E., Mavroukakis, S. A., Morre, M., Buffet, R., Mackall, C. L., and Gress, R. E. (2006) IL-7 administration to humans leads to expansion of $CD8^+$ and $CD4^+$ cells but a relative decrease of $CD4^+$ T-regulatory cells. *J. Immunother.* **29,** 313–319
54. Perales, M. A., Goldberg, J. D., Yuan, J., Koehne, G., Lechner, L., Papadopoulos, E. B., Young, J. W., Jakubowski, A. A., Zaidi, B., Gallardo, H., Liu, C., Rasalan, T., Wolchok, J. D., Croughs, T., Morre, M., Devlin, S. M., and van den Brink, M. R. (2012) Recombinant human interleukin-7 (CYT107) promotes T cell recovery following allogeneic stem cell transplantation. *Blood* **120,** 4882–4891
55. Chirifu, M., Hayashi, C., Nakamura, T., Toma, S., Shuto, T., Kai, H., Yamagata, Y., Davis, S. J., and Ikemizu, S. (2007) Crystal structure of the IL-15-IL-15Rα complex, a cytokine-receptor unit presented in *trans*. *Nat. Immunol.* **8,** 1001–1007
56. Ring, A. M., Lin, J. X., Feng, D., Mitra, S., Rickert, M., Bowman, G. R., Pande, V. S., Li, P., Moraga, I., Spolski, R., Ozkan, E., Leonard, W. J., and Garcia, K. C. (2012) Mechanistic and structural insight into the functional dichotomy between IL-2 and IL-15. *Nat. Immunol.* **13,** 1187–1195
57. Han, K. P., Zhu, X., Liu, B., Jeng, E., Kong, L., Yovandich, J. L., Vyas, V. V., Marcus, W. D., Chavaillaz, P. A., Romero, C. A., Rhode, P. R., and Wong, H. C. (2011) IL-15:IL-15 receptor α superagonist complex. High-level co-expression in recombinant mammalian cells, purification and characterization. *Cytokine* **56,** 804–810
58. DePaolo, R. W., Abadie, V., Tang, F., Fehlner-Peach, H., Hall, J. A., Wang, W., Marietta, E. V., Kasarda, D. D., Waldmann, T. A., Murray, J. A., Semrad, C., Kupfer, S. S., Belkaid, Y., Guandalini, S., and Jabri, B. (2011) Co-adjuvant effects of retinoic acid and IL-15 induce inflammatory immunity to dietary antigens. *Nature* **471,** 220–224
59. Gonzalez-Alvaro, I., Ortiz, A. M., Garcia-Vicuña, R., Balsa, A., Pascual-Salcedo, D., and Laffon, A. (2003) Increased serum levels of interleukin-15 in rheumatoid arthritis with long-term disease. *Clin. Exp. Rheumatol.* **21,** 639–642
60. Rentzos, M., Cambouri, C., Rombos, A., Nikolaou, C., Anagnostouli, M., Tsoutsou, A., Dimitrakopoulos, A., Triantafyllou, N., and Vassilopoulos, D. (2006) IL-15 is elevated in serum and cerebrospinal fluid of patients with multiple sclerosis. *J. Neurol. Sci.* **241,** 25–29